ACS Biomaterials SCIENCE & ENGINEERING

Article

pubs.acs.org/journal/abseba

Highly Elastic and Moldable Polyester Biomaterial for Cardiac Tissue Engineering Applications

Locke Davenport Huyer,[†,‡] Boyang Zhang,[†,‡] Anastasia Korolj,[†,‡] Miles Montgomery,[†,‡] Stasja Drecun,[§] Genevieve Conant,[†,‡] Yimu Zhao,[†] Lewis Reis,[‡] and Milica Radisic*[,†,‡]

[†]Department of Chemical Engineering and Applied Chemistry, [‡]Institute of Biomaterials and Biomedical Engineering, and [§]Human Biology, University of Toronto, Toronto, Ontario, Canada

Supporting Information

ABSTRACT: Polyester biomaterials are used in tissue engineering as scaffolds for implantation of tissues developed in vitro. An ideal biodegradable elastomer for cardiac tissue engineering exhibits a relatively low Young's modulus, with high elongation and tensile strength. Here we describe a novel polyester biomaterial that exhibits improved elastic properties for cardiac tissue engineering applications. We synthesized poly(octamethylene maleate (anhydride) 1,2,4-butanetricarboxylate) (124 polymer) prepolymer gel in a one-step polycondensation reaction. The prepolymer was then molded as desired and exposed to ultraviolet (UV) light to produce a cross-linked elastomer. 124 polymer exhibited highly elastic properties under aqueous conditions that were tunable according to the UV light exposure, monomer composition, and porosity of the cured elastomer. Its elastomeric properties fell within the range of adult heart myocardium, but they could also be optimized for higher elasticity for weaker immature constructs. The polymer showed relatively stable degradation characteristics, both hydrolytically and in a cellular environment, suggesting maintenance of material properties as a scaffold support for potential tissue implants. When assessed for cell interaction, this polymer supported rat cardiac cell attachment in vitro as well as comparable acute in vivo host response when compared to poly(L-lactic acid) control. This suggests the potential applicability of this material as an elastomer for cardiac tissue engineered constructs.

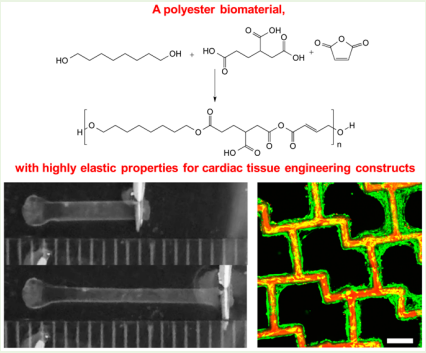

KEYWORDS: *elastomer, regenerative medicine, tunable properties, biodegradable, microfabrication, cross-linkable*

INTRODUCTION

Engineered tissue constructs rely on biomaterial polymers as support structures for tissue construction.[1] These materials form a support mechanism that assist immature groups of cells to develop into complex tissue networks that exhibit the properties of native cells, and support the integration of these complexes into the host surroundings.[2,3] It is important that these polymers mimic the physical properties of the host tissue, have appropriate degradation properties, and limit host response.[4] Recently, the tissue engineering community has increasingly focused on the utilization of polyester biomaterials for scaffold construction.[5] These polymers are desirable for their simple synthesis procedure, hydrolytic degradation properties, and elastomeric characteristics. There has been a number of notable applications of polyester materials in FDA approved products, including polycarprolactone and poly-L-lactic acid, but the high stiffness of these materials limits their use in soft tissue scaffolds.[6,7] These limitations have directed synthesis efforts toward developing materials exhibiting more elastic properties.

Biomaterial based cardiac tissue engineering solutions rely on optimized material properties which mimic the properties of native cardiac tissue for effective development of tissue constructs.[8] Many criteria must be considered including elasticity, degradation rate, and material compatibility in vivo.[8,9] Materials used for cardiac tissue engineering are difficult to optimize. Ventricular filling and ejection leads to repetitive cyclic loading on the material construct which they must withstand while ensuring they do not constrict the tissue to which support is being provided.[9] Therefore, matching the mechanical properties of the heart is important. The human heart has a Young's modulus that varies from 10 to 20 kPa at the beginning of diastole to 200−300 kPa at the end of systole.[10−13] Immature engineered cardiac tissue constructs tend to exhibit a lower force of contraction, so a more elastic material is desirable to support the development of contractile apparatus.[14,15] It is important that properties match this elasticity, as those that are too stiff can be found to restrict tissue contraction.[16−18] Therefore, an ideal biodegradable elastomer for cardiac tissue engineering should exhibit a relatively low Young's modulus, with high elongation and tensile strength.[9] Furthermore, the material should exhibit degradation properties that allow the breakdown of the scaffold in vivo over a 6−8 week period to support engineered tissue integration with the host but not restrict continued regeneration.[4,19] Finally, materials must be

Received: December 7, 2015
Accepted: April 13, 2016
Published: April 28, 2016

DOI: 10.1021/acsbiomaterials.5b00525
ACS Biomater. Sci. Eng. 2016, 2, 780−788

compatible with the immune system of the host, as inflammatory and immune response to tissue engineering constructs greatly limits their regenerative potential.[20,21]

An ideal polymer should be an elastomer constructed of biocompatible monomers and prepared via a simple synthetic route. We focused on a two-step elastomer preparation process with incorporation of photocuring moieties to develop a final cross-linked structure. This enables molding of a prepolymer gel into complex shapes needed for cardiac tissue engineering, where the final function of the tissue is strongly determined by its structure. Furthermore, we looked to ensure the elastomeric properties mimicked those of human adult myocardium, and the material exhibited characteristics for appropriate use both in vitro and in vivo.

In this paper, we describe an approach for rational design of cardiac tissue engineering elastomers, results of their toxicity testing followed by a full characterization of the most promising candidate, poly(octamethylene maleate (anhydride) 1,2,4-butanetricarboxylate) (124 polymer). This material was synthesized through a one-step polycondensation of 1,8-octanediol, 1,2,4-butanetricarboxylic acid and maleic anhydride. We also provide characterization of its mechanical properties, degradation rate and cell compatibility both in vitro and in vivo.

EXPERIMENTAL SECTION

124 Polymer Synthesis. The first step in material development was synthesis of polyester prepolymer. 1,8-octanediol (Sigma), maleic anhydride (Sigma), and 1,2,4-butanetricarboxylic acid (Sigma) were combined in a 250 mL round-bottom flask under nitrogen flow. The ratio of hydroxyl to carboxylic acid end groups were kept at a 1:1 ratio to allow for complete reaction of chemically active sites while the ratio of 1,2,4-butanetricarboxylic acid to maleic anhydride was varied. Monomers were melted and stirred at 150 °C with stirring at 200 rpm for 4 h. The crude prepolymer solution was then dissolved in 1,4-dioxane (Sigma) and dripped through deionized distilled water. The water was decanted and the purified prepolymer was collected and dried under constant airflow for 48 h (Yield: 76%). The purified prepolymer was mixed with 5 wt % UV initiator (2-hydroxy-1-[4(hydroxyethoxy)-phenyl]-2-methyl-1 propanone, Irgacure 2959, Sigma) by heating above 100 °C and allowing the initiator powder to fully mix in the polymer solution. When appropriate, poly(ethylene glycol) dimethyl ether (PEGDM, Sigma) was added as a porogen to the solution at the desired concentration (wt %). The porogen was leached out in Dulbecco's phosphate buffered saline (PBS, Gibco) post UV cross-linking to make a nanoporous structure. Alternatively, tartaric acid or malic acid were used in lieu of 1,2,4-butanetricarboxylic acid using the procedure described above. Final polymer structures were developed through exposure to ultraviolet light (365 nm) on a OAI Hybralign Series 200 mask aligner with a 2105C2 Illumination controller. Light intensity (~15 mW/cm^2) was measured before each exposure and used to tune the exposure time to the desired exposure energy.

POMaC Prepolymer Synthesis. POMaC prepolymer was synthesized as previously described.[22] Briefly, 1,8-octanediol, maleic anhydride, and citric acid (Caledon) were combined and melted under nitrogen flow. Polycondensation was carried out and a purified concentrated prepolymer was obtained. Final elastomeric structures were developed with mixing of prepolymer geI with UV initiator and exposure to UV light according to application. When appropriate, nanoporous structures were developed with mixing of porogen with the prepolymer gel.

Characterization of Polymer Properties. Polymer structure was confirmed using ^{1}H NMR on an Agilent DD2 600 MHz spectrometer. Polymer samples were dissolved in deuterated dimethyl sulfoxide (DMSO-d_6, Sigma). Chemical shifts were tested against the resonance of protons in internal tetramethylsilane (TMS).

Contact angle was measured by sessile drop method (deionized water) in air using a Goniometer (Ramé-hart Model 100−00) modified with a digital microscope incorporated for image acquisition (resolution 640 × 480 pixels grayscale) and a Ramé-hart HPLC straight needle, size 22G, attached to a 2 mL Gilmont microsyringe. Angles were manually measured on both sides of the drop and averaged.

Scanning Electron Microscopy. SEM was used to assess the nanoporous structure of cross-linked polymer material, using a Hitachi SEM S-3400 in secondary electron mode at the Microscopy Imaging Laboratory, Faculty of Medicine, University of Toronto. Before imaging, cross-linked polymer strips with and without 40% (m/m) initial PEGDM porogen content were soaked in deionized distilled water overnight, followed by lyophilization for 24 h.

Neonatal Rat Heart Cell Isolation. Neonatal rat heart tissue was digested as previously described.[23] In short, neonatal (1−2 day old) Sprague−Dawley rats (Charles River) were euthanized, and excised hearts were collected in Ca^{2+}, Mg^{2+} free Hank's balanced salt solution (HBSS) (Gibco). The aorta and vena cava structures were removed from the hearts, which were then quartered. The heart sections were rinsed twice in ice cold HBSS, then digested overnight (4 °C) in a solution of 0.06% (w/v) trypsin (Sigma) in HBSS. Further digestion was done using collagenase II (Worthington, 200 U/ml) in HBSS (37 °C) in five sets of 4−8 min digestions. Following digestion, cells were preplated for 40 min and the nonadherent cells were collected and used as the rat cardiomyocyte (CM) population. Rat CMs were cultured in Dulbecco's modified Eagle's medium (Gibco) containing glucose (4.5 g/Liter), 10% (v/v) fetal bovine serum (FBS; Gibco), 1% (v/v) Hepes (100 U/ml; Gibco), and 1% (v/v) penicillin-streptomycin (100 mg/mL; Gibco).

Mechanical Characterization. 124 polymer's Young's modulus was characterized through tensile testing. A three-factor design of experiment (DOE) was conducted to evaluate the range of moduli that 124 polymer can achieve as a result of variations in the preparation procedure. The three factors considered were: (A) monomer feed ratio of 1,2,4-butanetricarboxylic acid and maleic anhydride (124:MA), (B) UV exposure energy dose (mJ) and (C) porous fraction, achieved by the incorporation of porogen into the prepolymer which is leached out after curing. Following standard practice for DOE, these variables were coded using a general equation where x is an arbitrary variable (eq 1).

$$x_{\text{coded}} = \frac{x_{\text{uncoded}} - \bar{x}_{\text{uncoded}}}{\frac{1}{2}\text{range}(x_{\text{uncoded}})} \quad (1)$$

This general equation was used to code the high and low values (eqs 2-4), and the associated values are summarized in Table 1.

$$A = \frac{(a - 0.875)}{0.625} \quad (2)$$

$$B = \frac{(b - 18000mJ)}{9000mJ} \quad (3)$$

$$C = \frac{(c - 20\%)}{20\%} \quad (4)$$

The factors were varied at high and low levels yielding $2^3 = 8$ samples, plus replicates at a midpoint, as outlined in Table 2.

Batches of prepolymer were prepared according to the design matrix. A prepolymer was injected into a polydimethylsiloxane mold before the curing step, where each sample was then individually exposed to the experiment-prescribed UV exposure energy dose. Samples were designed as thin strips (length, 10 mm; width, 1.5 mm; thickness, 0.1 mm) suitable for tensile testing on a Myograph (Kent Scientific). Samples were collected and soaked in PBS for a minimum of 24 h before

Table 1. Summary of Maximum and Minimum Values for the Experimental Design

coded value	monomer ratio (124:MA)	UV exposure energy (mJ)	porogen content (%)
−1	0.25	9000	0
1	1.5	27000	40
0	0.875	18000	20

DOI: 10.1021/acsbiomaterials.5b00525
ACS Biomater. Sci. Eng. 2016, 2, 780−788

Table 2. Design Matrix for 1,2,4-Polymer's 2^3 Factorial Experiment with Two Midpoints

sample	monomer ratio (124:MA)	UV exposure energy (mJ)	porogen content (%)
1	1	1	1
2	−1	1	1
3	−1	−1	1
4	1	−1	1
5	1	1	−1
6	−1	1	−1
7	1	−1	−1
8	−1	−1	−1
replicates	−0.333	0	0

tensile testing, and tensile tests were conducted in PBS. Young's modulus was taken as the slope of the linear portion of the generated stress−strain curve and the test was carried out to failure.

Transwell Assay for Polymer Degradation. Prepolymer strips (124, POMaC, 124 + 40% porogen, POMaC + 40% porogen) (1.5 mm × 0.5 mm × 10 mm) were exposed to UV (365 nm) energy. The strips were weighed in sets of 8 to determine the initial mass. Strips were soaked in PBS for 2 h, 70% ethanol overnight, and washed twice with sterile PBS. These were then placed in the bases of transwell insert 24-well plates (Corning), with rat-CM seeded in the transwell inserts and cultivated in rat CM media. The strips were collected at days 1 and 14, washed twice in deionized distilled water and dried under lyophilization for 2 days. Final mass was measured, recorded, and expressed as a percentage loss of the initial dry mass (day 0). Strips were also characterized for a change in mechanical properties, as described in the Mechanical Characterization section above.

Hydrolytic Degradation. UV cured polymer strips, as described in "transwell degradation" above, were placed in preweighed 20 mL glass scintillation vials in sets of 8 and the initial dry mass was recorded. Ten milliliters of PBS was added to each vial, and each was sealed and placed in a 37 °C environment under agitation. Vials were collected at days 1, 7, 30, and 60; dried under lyophilization for 2 days; and the final dry mass was recorded. Degradation was reported as percentage of initial mass lost.

Cell Seeding on Mesh Patches. Cells were seeded on mesh patch designs previously described.[24,25] Briefly, a mesh design was fabricated using standard SU-8 photolithography techniques. The silicon wafer with the microfabricated scaffold design served as mold to generate a PDMS negative, which was injected with 124 polymer material with 40% initial porogen content (Figure S5). These scaffolds were cross-linked with UV light, soaked in PBS for porogen leaching, and 70% ethanol (sterile filtered) for sterilization. Following wash in PBS, scaffolds were coated with 0.2% (wt) gelatin in PBS (37 °C) for 3 h to assist in cell attachment. Freshly isolated rat CMs were first pelleted and suspended in liquid Matrigel solution (1 million cells/1uL Matrigel). Two microliters of cell suspension were pipetted onto the mesh surface, placed in a well of a 6 well plate (1 mesh/well). Excess cell was removed to ensure only a thin layer of cell solution covered each mesh. The well plates with the scaffolds were incubated (37 °C, 4−6 min) to allow for partial gelation. Rat culture media (3 mL/well, 37 °C) was then added to the plates, and mesh scaffolds were gently scraped from the bottom of the plate and allowed to float. Cell culture media was changed every 48 h for 7 days. Immuno-fluorescent staining was performed by first fixing the tissues at room temperature for 15 min in 4% (w/v) paraformaldehyde in PBS. Cells were then permeated and blocked in 10% FBS and 0.25% Triton X100 in PBS for 1 h. Tissues were then incubated in primary antibody against Troponin T (Mouse, Thermofisher, MS295P1) at 4 °C overnight, which was followed with secondary antibody incubation, TRITC antimouse IgG (Life Technologies, A21202) and a phalliodin 66 conjugated anti-F-actin (Life Technologies, A22285). A second set of meshes were incubated in primary antibody against Connexion 43 (Rabbit, Abcam, AB11370) at 4 °C overnight, followed by secondary antibody incubation, TRITC antirabbit IgG and a phalliodin 66 conjugated anti-F-actin. Meshes were also assessed for tissue viability of rat cardiomyocytes visually with CFDA-SE (1:1000, Life Technologies, C1157) and PI (Life Technologies, P5366) in PBS for 30 min at 37 °C, and were fixed in 10% formalin post staining. All tissues were then imaged with confocal microscopy (Olympus FV5-PSU confocal with IX70 microscope, Canada).

In Vivo Study. 124 polymer, POMaC, and poly(L-lactic acid) (PLLA) (as relative control) discs (8 mm (d) × 1.5 mm (t)) were used to assess in vivo host response. 124 polymer discs and POMaC were prepared from prepolymer with a 2:3 ratio of 124-butanetricarboxylic acid to maleic anhydride and cured with 54000 mJ/cm^2 of UV energy. PLLA (Sigma) discs were cast in chloroform (Sigma) and the solvent was removed. Discs were sterilized in 70% ethanol and washed twice in sterile PBS. Discs were implanted subcutaneously in the back of Lewis rats (Charles River). Implantation side and order was randomized to ensure independence. Rats with 124 polymer (n = 4), POMaC (n = 4), and PLLA (n = 5) disc implants were euthanized 7 days post-implantation. Additional rats with 124 polymer (n = 5) and PLLA (n = 5) implants were euthanized 60 days postimplantation. Tissue surrounding the discs was excised and fixed in 10% formalin for 24h. Samples were then placed in PBS and sent for paraffin-embedding and sectioning at the Pathology Research Program (University Health Network, Toronto, ON). All samples were stained for Masson's Trichrome, CD68, CD163, and CD3. Samples from the 60 day experiment were additionally stained for CD31, and smooth muscle actin (SMA). Cell presence was assessed as a percentage of total area (400 pixels from implant edge) with positive stain.

Statistical Analysis. The error bars in figures are representative of standard deviation. Analysis was conducted using SigmaPlot 12. Normality and equality of variance was tested and the appropriate test was selected for each data set. Statistical analysis in Figure 2 was done with a Student's t test. Analysis in Figures 3 and 6 and Figure S4 was done by one-way ANOVA followed by a Tukey-Kramer test. In Figure 4 and Figure S2, two-way ANOVA was used followed by Shapiro-Wilk test.

RESULTS AND DISCUSSION

Rationale for Monomer Selection and the Approach to Synthesis. Development of the elastomeric material for cardiac tissue engineering relied on four design criteria: (a) A simple synthesis procedure that utilizes monomers that are both cost-effective and regarded as safe in their singular form; (b) possession of highly tunable mechanical properties which fall within the range of human cardiac tissue; (c) the ability to serve as a scaffold material for cardiac cells in vitro; and (d) the presentation of minimal host response with subcutaneous implantation.

Motivated by the previously described and well characterized elastomeric material poly(octamethylene maleate (anhydride) citrate) (POMaC),[24] we used a polycondensation synthesis technique. This material provides many of the properties desired for functional tissue engineering applications;[22] however, it is limited by its elasticity for cardiac tissue engineering use (elongation, 194%; Young's modulus, 290 kPa; Tensile Strength, 611 kPa).[22] With this in mind, we looked to synthesize a novel material that improved on the elastomeric properties for the purpose of cardiac tissue engineering.

To prepare a polyester material, it was necessary to react an alcohol with an acid. Thus, we collected a list of diol and carboxylic acid candidates for potential synthesis. Initial screening was conducted in literature to assess the toxicity of each monomer, and those that were not regarded as safe were eliminated. We then performed polymerization of tartaric acid and malic acid (in two separate trials) in a copolymer with 1,8 octanediol and maleic anhydride. Both of these results proved unsuccessful. Tartaric acid polymer exhibited cytotoxic effects when exposed to rat cardiac fibroblasts, which was attributed to

DOI: 10.1021/acsbiomaterials.5b00525
ACS Biomater. Sci. Eng. 2016, 2, 780−788

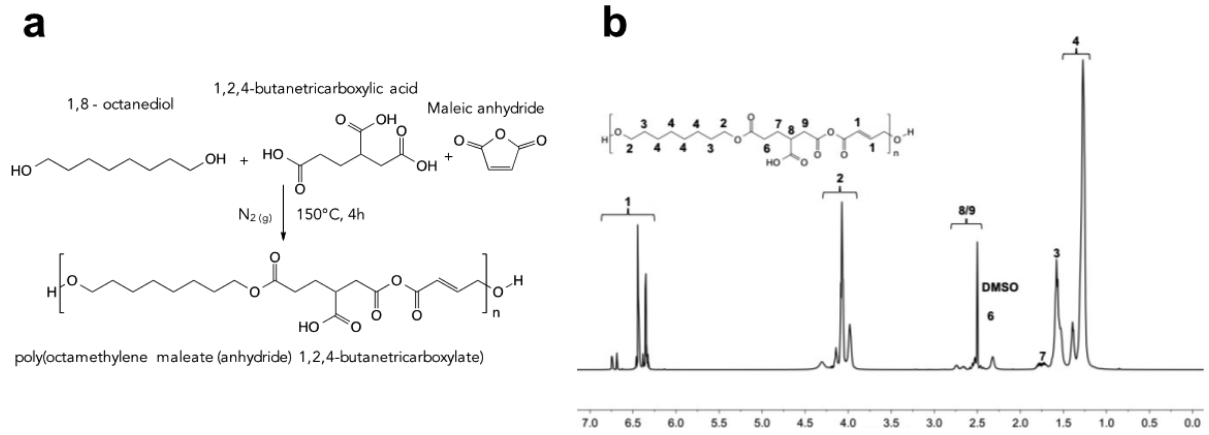

Figure 1. Structural characterization of 124 prepolymer. (a) 1,8-octanediol, 1,2,4-butanetricarboxylic acid and maleic anhydride underwent polycondensation (T = 150 °C) under a nitrogen atmosphere to generate a viscous 124 prepolymer fluid. (b) Representative ^{1}H NMR for 124 prepolymer fluid.

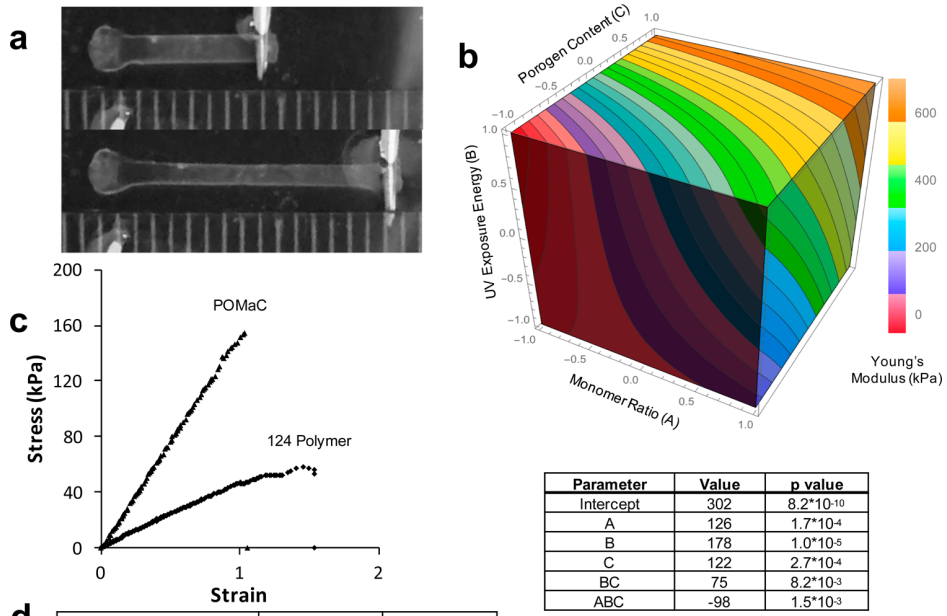

Parameter	Value	p value
Intercept	302	8.2*10-10
A	126	1.7*10-4
B	178	1.0*10-5
C	122	2.7*10-4
BC	75	8.2*10-3
ABC	-98	1.5*10-3

d

	124 Polymer	POMaC
Young's Modulus	44 ± 7kPa	218 ± 56kPa
Ultimate Tensile Strength	34 ± 13kPa	154 ± 16kPa
Elongation at Break	99 ± 32%	80 ± 16%

Figure 2. Assessment of 124 polymer mechanical properties. (a) Demonstration of 124 polymer material elastic stretch (scale in mm). (b) Mathematical representation of Young's Modulus to monomer ratio (A), UV exposure energy (B), and porogen content (C). The 3D heat plot is a graphical representation of eq 5. The model incorporates the parameters shown in the table above, incorporating statistically significant ($p < 0.05$) main and interaction factors. (c) Stress−strain curve of 124 polymer compared to POMaC under the same synthesis conditions. 124 polymer exhibits a more gradual slope, demonstrating more elastic characteristics. (d) Summarized elastomeric properties of 124 polymer and POMaC under the same synthesis conditions.

its properties as a Krebs cycle inhibitor.[26] Furthermore, malic acid polymer was unable to form sufficient cross-links to serve as an elastomeric material. Without branching in the prepolymer material (i.e., linear prepolymer), we found there was a reliance on UV cross-linking to produce the final elastomer, making it difficult to achieve desirable properties. These findings suggested it was necessary to maintain the uneven ratio of functional groups of, e.g., 2:3, in order to enable branching and cross-linking of linear polymer chains. Thus, we created a list of diol candidates that would be reacted with candidate tricarboxylic acids. Alternatively, triols could be reacted with dicarboxylic acids. This lead us to the synthesis of 124 polymer, a tricarboxylic-acid monomer reacted with a diol candidate.

Characterization of 1,2,4-Polymer. Polycondensation of 1,2,4-butanetricarboxylic acid, maleic anhydride and 1,8-octanediol under nitrogen conditions yielded a viscous yellow prepolymer gel (Figure 1a). For assessment of synthesis, polymers were reacted in a 2:3 molar ratio of 1,2,4-butanetricarboxylic acid to maleic anhydride, while maintaining an equal number of carboxylic acid to hydroxyl reaction sites. The water-in-air contact angle was assessed as 84.5°, which is comparable to POMaC (82.4°) and higher than other common polyesters such as poly(glycerol sebacate) (32.0°), suggesting

DOI: 10.1021/acsbiomaterials.5b00525
ACS Biomater. Sci. Eng. 2016, 2, 780−788

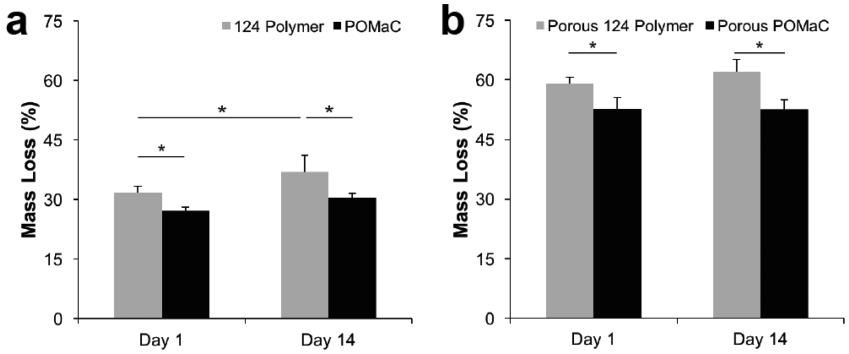

Figure 3. Mass loss of polymers in a transwell plate environment with rat cardiomyocytes for evaluation of cellular effects on polymer degradation. Change in mass of photo-cross-linked 124 polymer and POMaC was observed in (a) their pure form and (b) with 40% (m/m) initial porogen content over a 14 day period at 37 °C (*$p < 0.05$, $n = 5$).

relatively hydrophobic surface properties in comparison.[27] The relatively low viscosity allows for prepolymer injection through typical needle gauges, allowing for molding into microfabricated structures prior to UV exposure.

The structure of this polymer gel was verified with resonance of hydrogen atoms. Figure 1b presents a representative ^{1}H NMR spectrum for 124 prepolymer. Peak assignment was conducted with respect to tetramethylsilane (TMS). The peaks (1) between 6 and 7 ppm were assigned to the −CH═CH− bonds incorporated into the polymer backbone. The peaks (2) in the range of 3.75−4.5 ppm are assigned to $-O-CH_2$ in the 1,8-octanediol portion of the backbone. Peaks (3,4) (1.27, 1.39,1.58 ppm) are assigned to the CH_2-CH_2 bonds from 1,8-octanediol and the variation in shift is attributed to the proximity to the ester bond. The peaks (6−9) at 1.79 ppm and 2.32−2.74 ppm are attributed to the CH_2-CH_2 and the CH_2 bonded to ester or carboxylic acid groups. The high number of peaks in this structure is attributed to the variation in random polymer structure and degree of branching, causing slight shifts in peak location.

Elastic Modulus Testing. UV cross-linked 124 polymer material demonstrated highly elastic properties (Figure 2a). Using a statistical design of experiments, the relationship between UV exposure energy, monomer feed ratio, and porogen content on the Young's modulus of photo-cross-linked 124 polymer was investigated. This 2^3 factorial design method allows for coding of the variables within a minimum and maximum for the model, and therefore simplifying the mathematical assessment through removal of units and varying magnitude of variables.[28] Figure 2b shows a graphical and mathematical representation of this relationship, and the associated coded variables for this study can be found in Tables 1 and 2. Statistical assessment ($p < 0.05$) was used to remove interaction factors for monomer ratio with UV exposure energy and porogen content. This experimental design developed a mathematical model relating Young's modulus (E) to the independent factors and their interactions as follows (eq 5):

$$E\ (\text{kPa}) = 302 + 126A + 178B + 122C + 75BC - 98ABC \quad (5)$$

where A,B, and C are coded variables for monomer ratio, UV exposure energy (mJ) and porogen content (%) respectively. This model has increased accuracy with modulus values greater than 100 kPa, as testing at the low extremes of UV exposure energy (−1) and monomer ratio (−1) utilized a material with fluid-like properties.

A positive relationship was observed between each of the individual factors and the modulus of the cross-linked material. This supports the associated chemical theory. The increase in 1,2,4-butanecarboxylic acid content over maleic anhydride increases the branched structure of the material, and in turn the viscosity and molecular weight of the prepolymer material. This increase in branched networks decreases the ease at which polymer chains can slide past each other in the polymer bulk, leading to increased stiffness. Increased UV exposure causes further photo-cross-linking, similarly decreasing elastic properties. It should be noted that we assessed the effect of UV cross-linking through the variation of exposure time, but this could also be varied according to photoinitiator content to maintain a constant exposure. Third, and as supported by the statistically significant interaction factor between UV exposure and porogen content, the addition of PEGDM localizes polymer cross-links. We suggest that while the addition of porogen to prepolymer generates a miscible polymer blend, it also gives localized pockets of 124 polymer material.[29] This was confirmed with SEM imaging (Figure S1), where observation of nanopores suggests the generation of a porous cross-linked elastomer structure postporogen leaching. Therefore, with additional porogen the effect of UV energy is intensified, giving a final material with a higher degree of cross-linking.

On the basis of the results of this modeling, a monomer ratio of 2:3 (acid: anhydride) was the focus of the remainder of analysis. The development of this mathematical model allows for the fine-tuning of the final polymer material for applications based on the desired scaffold elasticity. In cardiac tissue engineered solutions, this adaptability is highly desired, as there is a link between cellular behavior and the mechanical properties of their surroundings.[14] The values demonstrated suggest a high degree of elasticity of this material, falling within the range of typical human cardiac properties.[10−13] Furthermore, when compared to a POMaC control synthesized under comparable conditions, 124 polymer presented a lower Young's Modulus (Figure 2c, d), suggesting improved elastomeric characteristics. This is advantageous in cardiac tissue engineering applications, as contracting engineering cardiac tissue requires a highly elastic material to support the cyclic loading of supporting biomaterial scaffolds. Low Young's modulus is desired in order to enable unobstructed relaxation of the tissue at the end of contraction. Materials with high Young's modulus may impede diastolic properties of the tissue.

DOI: 10.1021/acsbiomaterials.5b00525
ACS Biomater. Sci. Eng. 2016, 2, 780−788

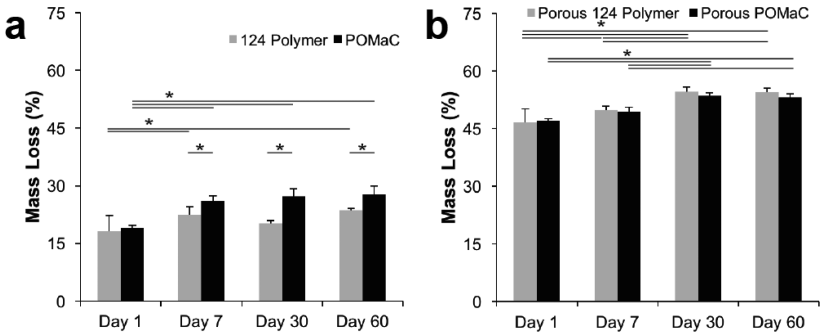

Figure 4. Mass loss of polymers in phosphate buffered saline solution. Changes in mass of photo-cross-linked 124 polymer and POMaC were observed in (a) pure form and (b containing 40% (m/m) initial porogen content) in PBS at 37 °C over a 60 day period (*$p < 0.05$, $n = 4$).

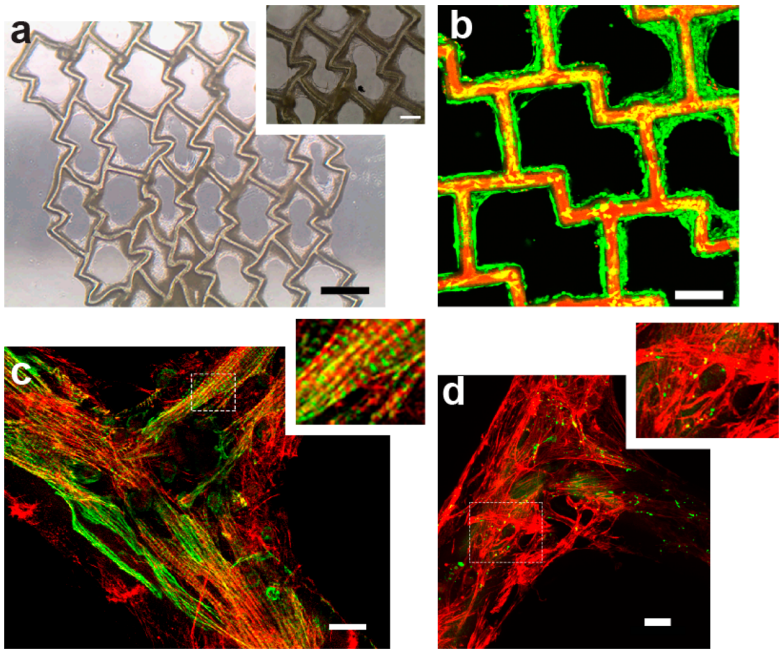

Figure 5. 124 polymer can be molded into elastic scaffolds and supports rat cardiac cell culture. Rat cardiac tissue was cultured for 7 days on 124 scaffold meshes. (a) A bright field image of the seeded scaffold at two different magnifications (scale bar, 250 μm (left), 100 μm (right)). (b) Live dead staining of rat cardiomyocytes (scale bar, 200 μm), where live cells are labeled green and dead cells are labeled red. The scaffold also exhibits autofluorescence in the red channel. (c) Staining of rat cardiomyocyte tissue constructs on 124 polymer scaffold (scale bar, 20 μm), where red is F-actin and green is cardiac troponin-T, presents the ability for cell attachment of rat cardiomyocytes. Magnified images present characteristic cross-striations of cardiac cells. (d) The physical connection of cardiac tissue is shown by Connexion 43 staining (green) at cellular junctions (scale bar, 20 μm).

Degradation. The mass loss and change in Young's modulus were assessed for photo-cross-linked 124 polymer samples both in phosphate-buffered saline and in transwell plates containing neonatal rat cardiomyocytes. This investigation further assessed the role of porosity, as degradation experiments were conducted with replicates with and without porogen content. The assessment utilized POMaC elastomer as a control, synthesized and UV exposed under similar conditions. The mass loss was assessed over 14 days in transwell conditions (Figure 3) and 2 months in PBS (Figure 4).

In this degradation assessment, we were able to determine the effects of both hydrolytic degradation mechanisms as well as potential differences when exposed to the enzymatic environment of cardiac cells. Over a 14 day period in a cellular environment, pure 124 polymer exhibited a slight increase in mass loss, which was of statistical significance but did not result in a large decrease in mass (Figure 3a). Similar results were observed when testing nanoporous material (Figure 3b). In both situations, the mass loss was greater than that of POMaC control ($p < 0.05$), but the magnitude of the difference was small. POMaC showed no appreciable mass loss over 14 days. The initial mass loss in pure materials is attributed to the soluble characteristics of low molecular weight chains of each material, and the additional mass loss of porogen containing materials is attributed to the leaching of water-soluble PEGDM.

Under hydrolytic degradation conditions in PBS, mass loss was nonsignificant in pure 124 polymer over 60 days, which contrasts greater degradation of statistical significance in POMaC control over the same period (Figure 4a). In samples with initial porogen content, hydrolytic degradation was more evident, with significant change in mass loss in each material over 60 day period (Figure 4b). In these instances, there was no difference between the 124 polymer and POMaC control. Similar to the transwell study, mass loss at 1 day is attributed to solubility and porogen leaching when appropriate. Under hydrolytic degradation conditions, the porogen content appears to effect the rate of

DOI: 10.1021/acsbiomaterials.5b00525
ACS Biomater. Sci. Eng. 2016, 2, 780−788

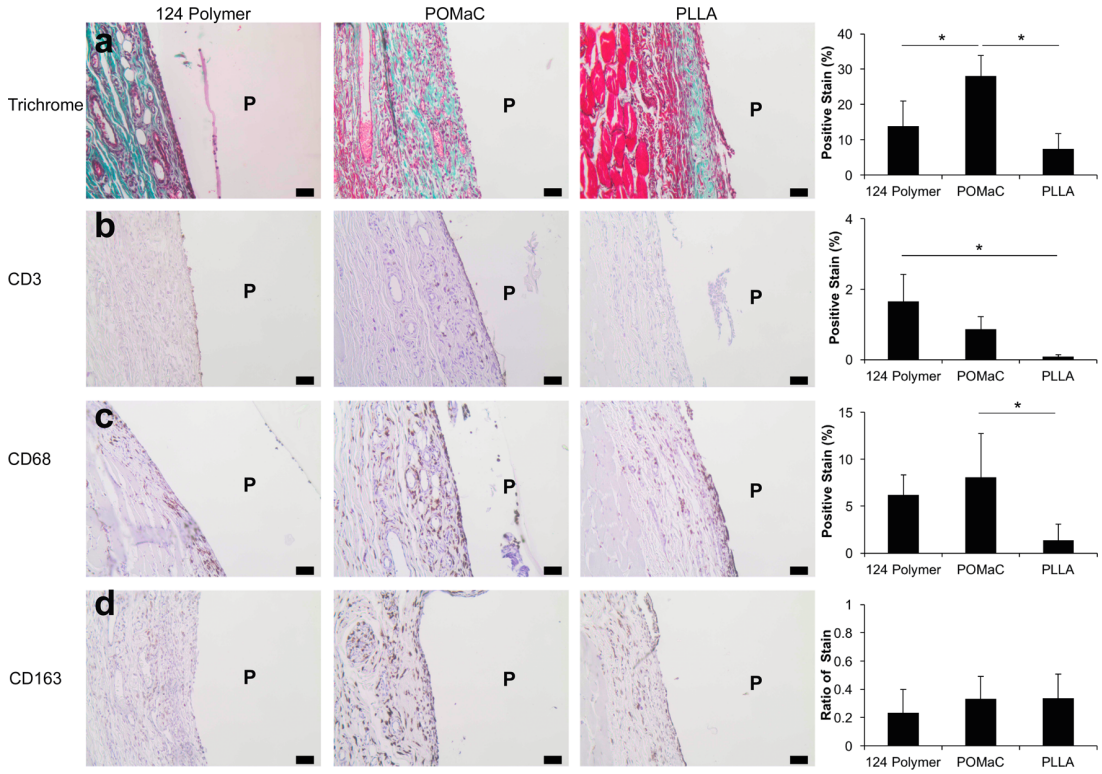

Figure 6. Photomicrographs of rat tissue explants which surrounded subcutaneous polymer discs of 124 polymer (left) POMaC (center) and PLLA (right) 7 days postimplantation. Images were stained for specific markers. All stains were quantified as percentage of total area with a positive stain (*p < 0.05, P = polymer disc) (a) Masson's Trichrome staining presents less collagen deposition along the 124 polymer disc boundary in comparison to POMaC and similar deposition to PLLA control. (b) T-cell recruitment (CD3) is heightened along 124 polymer sample boundaries compared to the PLLA control but with low absolute quantities, and similar to POMaC implants. (c) Staining for all macrophages (CD68) and (d) M2 macrophages (CD163) shows a similar response to controls (quantified as a ratio of CD163 to CD68 expression). Scale bars, 25 μm.

degradation. This suggests the porous structure allows for improved water penetration into the polymer bulk in both materials, causing appreciable mass loss from the polymer bulk. This property seems to play the opposite effect in the pure material. 124 polymer possesses a more hydrophobic polymer backbone on a molecular level. The limited degradation rate in comparison to the POMaC control could suggest diffusion limitations of water into the polymer bulk. Overall, 124 polymer degradation is relatively similar to that of POMaC control, and shows the ability to maintain structure over a 2 month period, which supports its applicability in tissue engineering constructs. Comparison between degradation samples in contact with cells to those that were not in contact with the cells shows a noticeably higher mass loss of 124 polymer, particularly over the first 24 h. This suggests the solution properties of rat cardiomyocyte growth media and ethanol sterilization may have increased the solubility of low molecular weight polymer chains. Mass loss is comparable to other published synthetic polyester elastomers. Poly(glycerol sebacate) (PGS)[27] presents 17% mass loss over 60 days and comparable results are seen in acrylated PGS (PGSA) (10% mass loss over 10 weeks).[30] In contrast, stiff polyesters such as PLLA tend to maintain mass stability, where only 10% mass loss is seen over 273 days.[31]

Co-current assessment was conducted on the change of Young's modulus as a measure of potential bulk erosion (Figure S2). There was no appreciable decrease in the Young's modulus of the samples tested, suggesting the material maintained mechanical properties over a 14 day and 2 month period for transwell and hydrolytic degradation conditions, respectively. This further supports potential applicability in tissue engineered constructs, as mechanical stability is an important aspect to structural support. Furthermore, this study allowed for a direct comparison of elastic properties of 124 polymer to those of POMaC. Our polymer exhibited a significantly lower Young's modulus than POMaC, both initially and over time, suggesting the material is more elastic. This could be attributed to the absence of the hydroxyl pendant group found on citric acid in POMaC, suggesting there may be a greater polymer chain length between entanglements. This improvement is desirable for support of cardiac tissue engineering constructs, as there is less potential for inhibition of contraction in immature tissues.

In Vitro Cell Attachment. Mesh scaffolds based on our previously published design[24] were injected with 124 prepolymer gel and photo-cross-linked to generate an elastomeric tissue engineering construct. Rat cardiomyocytes seeded on the scaffolds were assessed for cell survival through confocal imaging (Figure 5).

High cell survival 7 days postseeding is observed through live–dead staining (Figure 5c), demonstrating the noncytotoxic nature of 124 polymer constructs. Staining with cardiac troponin-T and F-actin and imaging by confocal microscopy demonstrated the formation of rat cardiomyocyte tissue on the engineered mesh (Figure 5b). Cross-striations (Figure 5b) and connexion 43 positive junctions (Figure 5d) were evident, further supporting the presence of intercellular connections and organized cardiac tissue. Corresponding bright-field imaging of these scaffolds (Figure 5a) shows tissue development around the accordion-like mesh repeating unit. This tissue demonstrated synchronous

DOI: 10.1021/acsbiomaterials.5b00525
ACS Biomater. Sci. Eng. 2016, 2, 780–788

beating under electrical stimulation 7 days post seeding (Movie S1). Real-time observation shows evident compression of the accordion scaffold design, suggesting the elastic properties of the material support the synchronous tissue contraction. The structural integrity of the tissue is maintained over this time period; tissue can be handled with forceps and maintain its scaffold shape and spontaneous beating (Movie S2). This analysis suggests the applicability of cross-linked 124 polymer as a tissue engineering scaffold, as it supports cell survival and tissue development in vitro. Furthermore, no significant differences in cytotoxicity were observed between the monolayers of cardiac fibroblasts cultivated with polymer in comparison to polystyrene controls (Figure S3). In other preliminary studies, we attempted to seed cells on uncoated 124 and POMaC polymer films and saw poor adhesion when compared to seeding on tissue culture polystyrene. We utilized a gelatin coating on tissue mesh scaffolds to improve cell adhesion, as it had efficacy in previous work.[24,32] The construction of these microfabricated structures with 124 polymer demonstrates the ability to mold this polymer into intricate shapes. As the material is fairly nonviscous and can be easily injected, molds of scaffolds such as those shown here on the 1 mm scale are constructed without solvent. This is an important feature for construction of solvent-free tissue engineering scaffolds with complex microscale features.

In Vivo Host Response. The acute in vivo host response to 124 polymer was assessed with subcutaneous implantation of cross-linked polymer discs (n = 5) against POMaC and PLLA control discs (n = 5) after 7 days in vivo (Figure 6). We further assessed the long-term response over a 60 day period (Figure S4) of 124 polymer against a PLLA control.

The inclusion of PLLA as a relative control in vivo allows for assessment of biocompatibility of the new material, as PLLA is generally regarded as a safe implant material.[33] Quantification of positive stain area (%) gives insight into the quantitative comparison of implant materials. Assessment of response 7-days post implantation indicated that 124 polymer presented a similar host response to POMaC and PLLA controls. Quantification was performed on collagen deposition (blue intensity in Masson's Trichrome staining), T-cell immune recruitment ($CD3^+$), total macrophage cell presence ($CD68^+$), and the proportion of M2 macrophages ($CD163^+$). No significant difference was observed when comparing 124 polymer to PLLA with respect to collagen deposition (Figure 6a) and total macrophage recruitment (Figure 6c). Furthermore, the presence of M2 macrophages, which have a phenotype that encourages tissue regeneration, was very similar among the three material groups (Figure 6d). An increased response to 124 polymer compared to PLLA control was observed with T-cell recruitment (Figure 6b), suggesting an increased adaptive immune response to the material. This is implicating for potential in vivo application, but the low absolute positive stain area and nonsignificant difference to POMaC control suggest the adaptive response may be minor. There was no significant difference in the acute host response between the 124 polymer and POMAC (Figure 6b–d), aside from the degree of fibrosis in which POMAC exhibited more abundant staining compared to the 124 polymer (Figure 6a).

Long-term assessment (60 days) against PLLA control further validated the potential application of 124 polymer in vivo. A significant difference was seen in the two materials for Masson's Trichrome, CD68 and CD3 staining (Figure S4a, b, d). Quantification shows an increased T-cell and macrophage recruitment along the implant boundary and a decreased collagen content in 124 polymer samples in comparison to the PLLA control. The deposition of dense collagen is an effort to segregate the implant, a final effort by the host to defend against the foreign object. Although we see an increased macrophage presence, we suggest the decreased collagen deposition signifies a less severe host response. Furthermore, although T-cell recruitment is observed, it was again in low amounts in both groups, suggesting the adaptive response is minimal. There was no appreciable difference observed in vascular cell markers (CD31, a marker of endothelial cells; SMA, a marker for smooth muscle cells and myofibroblasts), which are utilized to quantify vascularization of the surrounding tissue (Figure S4e, f). Additionally, the presence of M2 (pro-healing) macrophages, were also found in similar quantities between the two materials (Figure S4c). This suggests that the growth of the surrounding tissue postinflammation is occurring in a similar fashion in the 124 polymer as in the PLLA control.

CONCLUSIONS

In summary, we synthesized a new polyester biomaterial through a simple one-step polycondensation synthesis. 124 polymer exhibited highly elastic properties under aqueous conditions that were tunable according to the UV light exposure, monomer composition, and porosity of the cured elastomer. When compared to a POMaC control this material was significantly more elastic (Young's modulus) in PBS. The improved elastic properties are desired for cardiac tissue engineering applications, as the material could be less inhibitory of cardiac tissue contraction while also providing structural support for the engineered constructs. The polymer showed similar degradation properties to POMaC, both hydrolytically and in a cellular environment. When assessed for cell interaction, this polymer showed the ability for rat cardiac cell attachment as well as a similar acute in vivo host response with comparison to POMaC and PLLA. The highly elastic polyester could be molded and photo-cross-linked into a complex mesh structure with feature size on the order of tens of micrometers, demonstrating utility in cardiac tissue engineering constructs.

ASSOCIATED CONTENT

Supporting Information

The Supporting Information is available free of charge on the ACS Publications website at DOI: 10.1021/acsbiomaterials.5b00525.

SEM images of nonporous and porous cross-linked polymer, Young's modulus change over time, additional in vitro cytotoxicity assessment, long-term in vivo results, in depth description of design of experiments, and scaffold preparation technique (PDF)

Movie S1, 124 polymer tissue mesh with contracting cardiac tissue (AVI)

Movie S2, handling of 124 polymer tissue mesh (AVI)

AUTHOR INFORMATION

Corresponding Author

*E-mail: m.radisic@utoronto.ca.

Funding

This work is funded by the NSERC Steacie Fellowship to M.R., Canadian Institutes of Health Research (CIHR) Operating Grants (MOP-126027 and MOP-137107), NSERC Discovery Grant (RGPIN 326982–10), and National Institutes of Health Grant 2R01 HL076485. The authors acknowledge the Canadian

DOI: 10.1021/acsbiomaterials.5b00525
ACS Biomater. Sci. Eng. 2016, 2, 780–788

Foundation for Innovation, Project 19119, and the Ontario Research Fund for funding of the Centre for Spectroscopic Investigation of Complex Organic Molecules and Polymers. L.D.H. is supported by CIHR Canadian Graduate Scholarships-Masters. M.M. is supported by NSERC Vanier Graduate Scholarships. G.C. is supported by Ontario Graduate Scholarships.

Notes

The authors declare no competing financial interest.

■ ACKNOWLEDGMENTS

We thank A. Scarpone and E. Acosta for help with contact angle measurement.

■ REFERENCES

(1) Ulery, B. D.; Nair, L. S.; Laurencin, C. T. Biomedical Applications of Biodegradable Polymers. *J. Polym. Sci., Part B: Polym. Phys.* **2011**, *49* (12), 832−864.

(2) Zhao, Y.; Feric, N. T.; Thavandiran, N.; Nunes, S. S.; Radisic, M. The role of tissue engineering and biomaterials in cardiac regenerative medicine. *Can. J. Cardiol.* **2014**, *30*, 1307.

(3) Chen, Q.; Liang, S.; Thouas, G. A. Elastomeric biomaterials for tissue engineering. *Prog. Polym. Sci.* **2013**, *38* (3−4), 584−671.

(4) Reis, L. A.; Chiu, L. L.; Feric, N.; Fu, L.; Radisic, M. Biomaterials in myocardial tissue engineering. *J. Tissue Eng. Regener. Med.* **2016**, *10*, 11.

(5) Bouten, C. V.; Dankers, P. Y.; Driessen-Mol, A.; Pedron, S.; Brizard, A. M.; Baaijens, F. P. Substrates for cardiovascular tissue engineering. *Adv. Drug Delivery Rev.* **2011**, *63* (4−5), 221−41.

(6) Langer, R.; Tirrell, D. A. Designing materials for biology and medicine. *Nature* **2004**, *428* (6982), 487−492.

(7) Chan, B. P.; Leong, K. W. Scaffolding in tissue engineering: general approaches and tissue-specific considerations. *European spine journal: official publication of the European Spine Society, the European Spinal Deformity Society, and the European Section of the Cervical Spine Research Society* **2008**, *17* (Suppl 4), 467−479.

(8) Huyer, L. D.; Montgomery, M.; Zhao, Y.; Xiao, Y.; Conant, G.; Korolj, A.; Radisic, M. Biomaterial based cardiac tissue engineering and its applications. *Biomed. Mater.* **2015**, *10* (3), 034004.

(9) Radisic, M.; Park, H.; Gerecht, S.; Cannizzaro, C.; Langer, R.; Vunjak-Novakovic, G. Biomimetic approach to cardiac tissue engineering. *Philos. Trans. R. Soc., B* **2007**, *362* (1484), 1357−68.

(10) Nagueh, S. F.; Shah, G.; Wu, Y.; Torre-Amione, G.; King, N. M.; Lahmers, S.; Witt, C. C.; Becker, K.; Labeit, S.; Granzier, H. L. Altered titin expression, myocardial stiffness, and left ventricular function in patients with dilated cardiomyopathy. *Circulation* **2004**, *110* (2), 155−162.

(11) Weis, S. M.; Emery, J. L.; Becker, K. D.; McBride, D. J., Jr.; Omens, J. H.; McCulloch, A. D. Myocardial mechanics and collagen structure in the osteogenesis imperfecta murine (oim). *Circ. Res.* **2000**, *87* (8), 663−9.

(12) Coirault, C.; Samuel, J. L.; Chemla, D.; Pourny, J. C.; Lambert, F.; Marotte, F.; Lecarpentier, Y. Increased compliance in diaphragm muscle of the cardiomyopathic Syrian hamster. *J. Appl. Physiol. (1985)* **1998**, *85* (5), 1762−1769.

(13) Omens, J. H. Stress and strain as regulators of myocardial growth. *Prog. Biophys. Mol. Biol.* **1998**, *69* (2−3), 559−72.

(14) Marsano, A.; Maidhof, R.; Wan, L. Q.; Wang, Y.; Gao, J.; Tandon, N.; Vunjak-Novakovic, G. Scaffold stiffness affects the contractile function of three-dimensional engineered cardiac constructs. *Biotechnology progress* **2010**, *26* (5), 1382−90.

(15) Park, H.; Radisic, M.; Lim, J.; Chang, B.; Vunjak-Novakovic, G. A novel composite scaffold for cardiac tissue engineering. *In Vitro Cell.Dev.Biol.-Animal* **2005**, *41* (7), 188−196.

(16) Chuong, C. J.; Sacks, M. S.; Templeton, G.; Schwiep, F.; Johnson, R. L., Jr. Regional deformation and contractile function in canine right ventricular free wall. *Am. J. Physiol.* **1991**, *260* (4 Pt 2), H1224−H1235.

(17) Rappaport, D.; Adam, D.; Lysyansky, P.; Riesner, S. Assessment of myocardial regional strain and strain rate by tissue tracking in B-mode echocardiograms. *Ultrasound Med. Biol.* **2006**, *32* (8), 1181−92.

(18) Sacks, M. S.; Chuong, C. J. Biaxial mechanical properties of passive right ventricular free wall myocardium. *J. Biomech. Eng.* **1993**, *115* (2), 202−205.

(19) Jawad, H.; Lyon, A. R.; Harding, S. E.; Ali, N. N.; Boccaccini, A. R. Myocardial tissue engineering. *Br. Med. Bull.* **2008**, *87*, 31−47.

(20) Griffith, L. G.; Naughton, G. Tissue engineering–current challenges and expanding opportunities. *Science* **2002**, *295* (5557), 1009−1014.

(21) Montgomery, M.; Zhang, B.; Radisic, M. Cardiac Tissue Vascularization: From Angiogenesis to Microfluidic Blood Vessels. *J. Cardiovasc. Pharmacol. Ther.* **2014**, *19* (4), 382−393.

(22) Tran, R. T.; Thevenot, P.; Gyawali, D.; Chiao, J. C.; Tang, L.; Yang, J. Synthesis and characterization of a biodegradable elastomer featuring a dual crosslinking mechanism. *Soft Matter* **2010**, *6* (11), 2449−2461.

(23) Radisic, M.; Park, H.; Shing, H.; Consi, T.; Schoen, F. J.; Langer, R.; Freed, L. E.; Vunjak-Novakovic, G. Functional assembly of engineered myocardium by electrical stimulation of cardiac myocytes cultured on scaffolds. *Proc. Natl. Acad. Sci. U. S. A.* **2004**, *101* (52), 18129−34.

(24) Zhang, B.; Montgomery, M.; Davenport-Huyer, L.; Korolj, A.; Radisic, M. Platform technology for scalable assembly of instantaneously functional mosaic tissues. *Sci. Adv.* **2015**, *1* (7), e1500423.

(25) Nunes, S. S.; Miklas, J. W.; Liu, J.; Aschar-Sobbi, R.; Xiao, Y.; Zhang, B.; Jiang, J.; Masse, S.; Gagliardi, M.; Hsieh, A.; Thavandiran, N.; Laflamme, M. A.; Nanthakumar, K.; Gross, G. J.; Backx, P. H.; Keller, G.; Radisic, M. Biowire: a platform for maturation of human pluripotent stem cell-derived cardiomyocytes. *Nat. Methods* **2013**, *10* (8), 781−7.

(26) Massey, V. Studies on fumarase. 4. The effects of inhibitors on fumarase activity. *Biochem. J.* **1953**, *55* (1), 172−177.

(27) Wang, Y.; Ameer, G. A.; Sheppard, B. J.; Langer, R. A tough biodegradable elastomer. *Nat. Biotechnol.* **2002**, *20* (6), 602−606.

(28) Montgomery, D. C.; Runger, G. C.; Hubele, N. F. *Engineering Statistics*; Wiley: New York, 2011.

(29) Hoshi, R. A.; Behl, S.; Ameer, G. A. Nanoporous Biodegradable Elastomers. *Adv. Mater.* **2009**, *21* (2), 188−192.

(30) Nijst, C. L. E.; Bruggeman, J. P.; Karp, J. M.; Ferreira, L.; Zumbuehl, A.; Bettinger, C. J.; Langer, R. Synthesis and Characterization of Photocurable Elastomers from Poly(glycerol-co-sebacate). *Biomacromolecules* **2007**, *8* (10), 3067−3073.

(31) Arias, V.; Hoglund, A.; Odelius, K.; Albertsson, A. C. Tuning the degradation profiles of poly(L-lactide)-based materials through miscibility. *Biomacromolecules* **2014**, *15* (1), 391−402.

(32) Zhang, B.; Montgomery, M.; Chamberlain, M. D.; Ogawa, S.; Korolj, A.; Pahnke, A.; Wells, L. A.; Masse, S.; Kim, J.; Reis, L.; Momen, A.; Nunes, S. S.; Wheeler, A. R.; Nanthakumar, K.; Keller, G.; Sefton, M. V.; Radisic, M. Biodegradable scaffold with built-in vasculature for organ-on-a-chip engineering and direct surgical anastomosis. *Nat. Mater.* **2016**, DOI: 10.1038/nmat4570.

(33) Gupta, B.; Revagade, N.; Hilborn, J. Poly(lactic acid) fiber: An overview. *Prog. Polym. Sci.* **2007**, *32* (4), 455−482.

DOI: 10.1021/acsbiomaterials.5b00525
ACS Biomater. Sci. Eng. 2016, 2, 780−788